Processing and Application of Ceramics 8 [3] (2014) 155–166
DOI: 10.2298/PAC1403155R

Influence of thermal treatment on the structure and *in vitro* bioactivity of sol-gel prepared $CaO\text{-}SiO_2\text{-}P_2O_5$ glass-ceramics

Lachezar Radev*

Department of Fundamental Chemical Technology, University of Chemical Technology and Metallurgy, 8, Kliment Ohridski Blvd., Sofia 1756, Bulgaria

Received 4 August 2014; Received in revised form 26 September 2014; Accepted 29 September 2014

Abstract

Nowadays there is a substantial practical interest in the in vitro bioactivity of calcium silicate phosphate (CSP) glass-ceramics and carbonate apatite (CO_3HA) formation on their surfaces after in vitro test in simulated body fluid (SBF). The main purpose of the presented article is the evaluation of the chemical composition of the gel with nominal composition 70.59 CaO:28.23 SiO_2:1.18 P_2O_5 (mol.%) on the structure, crystallization behaviour and in vitro bioactivity in SBF solution for 14 and 28 days. The prepared glass-ceramics have been synthesized via a polystep sol-gel method. The structure of the obtaining samples was studied by X-ray diffraction (XRD) analysis, Fourier transform infrared spectroscopy (FTIR) and scanning electron microscopy with energy dispersive X-ray spectroscopy (SEM-EDX). After thermal treatment of the samples XRD confirmed the presence of β-Ca_2SiO_4 and $Ca_{15}(PO_4)_2(SiO_4)_6$, and indicated that at 1500 °C $Ca_{15}(PO_4)_2(SiO_4)_6$ becomes predominant phase. FTIR revealed the presence of all characteristics bands for calcium silicate phosphate (CSP) bonds. SEM monitors the presence of particles with different morphology. After in vitro test in SBF, FTIR depicted that B-type carbonate containing hydroxyapatite (CO_3HA) is preferentially formed on the immersed glass-ceramics. SEM of the precipitated layers showed the presence of HA spheres. The changes in SBF solution after soaking the samples were recorded by inductively coupled plasma atomic emission spectroscopy (ICP-AES).

Keywords: *biomaterials, $Ca_{15}(PO_4)_2(SiO_4)_6$, β-Ca_2SiO_4, glass-ceramics, in vitro bioactivity*

I. Introduction

It is well known that hydroxyapatite, HA ($Ca_{10}(PO_4)_6(OH)_2$) exhibits beneficial properties as biomaterial, such as biocompatibility, osteoconductivity and good ability to bond directly to bone [1]. It is also known that HA shows a limited *in vitro* and *in vivo* reactivity. To solve this problem many research groups synthesized silicon substituted HA, Si-HA [2–7], due to the known role and influence of silicon on the new bone formation [8]. Based on these observations, some researchers [9,10] suggested that the HA forming ability at different glass-ceramics in $CaO\text{-}SiO_2\text{-}P_2O_5$ system could be measured in solutions of SBF, and the ability of biomaterials in formation of CO_3HA on the surface of the immersed samples.

In vitro bioactive glass-ceramics have been synthesized by our research team in two systems $CaO\text{-}SiO_2\text{-}P_2O_5$ [11] and $CaO\text{-}SiO_2\text{-}P_2O_5$-MgO [12] with different Ca/(P+Si) or (Ca+Mg)/(P+Si) molar ratio. On the basis of the obtained results we can summarize that $Ca_5(PO_4)_2SiO_4$ (silicocarnotite) was synthesized after thermal treatment at 1200 °C for 2 hours when molar ratio Ca/(P+Si) = 1.67, and $Ca_{15}(PO_4)_2(SiO_4)_6$ (calcium phosphate silicate), α-$CaSiO_3$ (wollastonite) and β-$CaSiO_3$ phases were denoted when Ca/(P+Si) = 1.89, [11]. Furthermore, in the case of MgO containing samples we produced two types of glass-ceramics as a function of (Ca+Mg)/(P+Si) molar ratio. When this ratio was 1.68 $Ca_2MgSi_2O_7$ (akermanite) and HA were observed. On the contrary, when this molar ratio was 2.16 $(Ca,Mg)_3(PO_4)_2$ (calcium magnesium phosphate) and $Ca_5(PO_4)_2SiO_4$ were detected [12]. It was also observed that the synthesized glass ceramics were *in vitro* bioactive after soaking in SBF solution in static conditions for different periods of time. In the other article [13]

*Corresponding author: tel: +35 92 816 3280
fax: +35 92 868 5488, e-mail: *l_radev@abv.bg*

we evaluated the relation between the quantity of P_2O_5 in the CaO-SiO_2-P_2O_5 system on the crystalline phases observed and for the *in vitro* bioactivity. On the basis of the experimental results we concluded that in the sample $Ca_{15}(PO_4)_2(SiO_4)_6$, Ca_2SiO_4 (dicalcium silicate) and $Ca_3(PO_4)_2$ (TCP) were observed. Briefly, in the CaO-SiO_2-P_2O_5 (MgO) systems, *in vitro* bioactive polycrystalline samples have been synthesized.

In the series of our papers, we also evaluated the possibility to obtain some *in vitro* bioactive composites between the synthesized glass-ceramics and some natural biodegradable polymers, such as collagen [14–16], gelatin [17,18], and fibroin [19]. Based on the obtained results it can be assumed that all synthesized composites exhibit good *in vitro* bioactivity, and they offer a promising way for creation of new bioimplants.

The aim of the presented study was to synthesize glass-ceramic in the CaO-SiO_2-P_2O_5 system and to evaluate their *in vitro* bioactivity in SBF solution for 14 and 28 days in static conditions.

II. Experimental

2.1. Materials

All chemicals used for modified sol-gel synthesis were reagent grade, tetraethylorthosilicate (TEOS, Fluka, Switzerland), calcium oxide (CaO, Merck, Germany), 85% phosphoric acid (H_3PO_4, Merck, Germany), 37% hydrochloric acid (HCl, Merck, Germany), 37% ammonia (NH_3, Merck, Germany). Ethanol (C_2H_5OH, Fluka, Switzerland) and deionized water, served as solvents in this study.

2.2. Sol-gel synthesis

The ceramic material in CaO-P_2O_5-SiO_2 system has been synthesized via polystep sol-gel method. The chemical composition of the prepared sol is described as 70.59 CaO:28.23 SiO_2 : 1.18 P_2O_5 (mol%). Sol A was obtained by appropriate amounts of $Ca(OH)_2$ and SiO_2. Silica sol was produced by prehydrolyzation of TEOS in the presence of C_2H_5OH, H_2O and HCl in molar ratio C_2H_5OH : H_2O : HCl = 1 : 1 : 4 : 0.01. $Ca(OH)_2$ was prepared by dissolution of CaO in deionized water under stirring. After recognizing the SiO_2 and $Ca(OH)_2$ solutions, $Ca(OH)_2$ was mixed "drop by drop" to the transparent SiO_2 sol under stirring. The obtained mixed sol A was intensively stirred for 4 hours. The sol B contains two components $Ca(OH)_2$ and H_3PO_4. As it was written above $Ca(OH)_2$ was obtained from CaO and deionized water in the appropriate amounts. The required amount of H_3PO_4 was added to $Ca(OH)_2$ solution carefully under stirring for 4 hours. 25% NH_4OH was used to obtain pH = 10–11 of mixed calcium phosphate (CP) solution. The sol B was added from the burette to the sol A under stirring for 20 hours to produce CSP solution. The obtained mixed sol was gelated at 120 °C for 12 hours and thermally treated at different temperatures (1200, 1300, 1400 and 1500 °C) for 2 hours. Thus, the synthesized samples were labelled as CSP 1200, CSP 1300, CSP 1400 and CSP 1500 in accordance with the temperature of treatment of the dried gels.

2.3. In vitro bioactivity test

Bioactivity of the obtained ceramic materials was evaluated by examining the apatite formation on their surfaces in SBF in accordance with Kokubo *et al.*

The SBF solution was prepared with 7.996 g NaCl, 0.350 g $NaHCO_3$, 0.224 g KCl, 0.228 g $K_2HPO_4 \times 3\,H_2O$, 0.305 g $MgCl_2 \times 6\,H_2O$, 0.278 g $CaCl_2$, 0.071 g Na_2SO_4, and buffering at pH = 7.4 at 36.5 °C with *TRIS* = 6.057 g and 1 M HCl in deionized water.

The synthesized ceramic powder was pressed at 50 MPa with PVA, as a binder, to obtain disc specimens (12 mm diameter and 2 mm thick) and immersed in SBF at the human body temperature (36.6 °C) in polyethylene bottles in static conditions for 14 and 28 days. A few drops of 0.5% sodium azide (NaN_3) were added to the SBF solution to inhibit the growth of bacteria [21,22]. After soaking, the specimens were removed from the fluid and gently rinsed with distilled water, and then dried at 36.6 °C for 12 h.

2.4. Characterization

The structure and *in vitro* bioactivity of synthesized glass-ceramics were monitored by XRD, FTIR and SEM.

XRD were collected within the range from 10 to 80° 2θ with a constant step 0.04° 2θ and counting time 1 s/step on Brucker D8 Advance diffractometer with Cu$K\alpha$ radiation and SolX detector. FTIR transmission spectra were recorded by using a Brucker Tensor 27 Spectrometer with scanner velocity 10 kHz. KBr pellets were prepared by mixing ~1 mg of the sample with 300 mg KBr. Transmission spectra were recorded using MCT detector with 64 scans and 1 cm^{-1} resolution.

SEM (SEM, Hitachi, TM3000) at an operating voltage of 15 kV and EDX were used to study morphology and Ca/(P+Si) ratio of the apatite formed on the surface of bioactive glass-ceramic samples.

The ion concentrations of Ca, P and Si before and after soaking in SBF for 14 and 28 days were recorded by ICP-AES using IRIS 1000, Thermo elemental, USA.

III. Results and discussion

XRD patterns of the synthesized sample, thermally treated at different temperatures, are given in Fig. 1.

In the sample treated at 1200 °C XRD confirmed the presence of crystalline maxima corresponding to β-Ca_2SiO_4 (PDF card 86-0398) and $Ca_{15}(PO_4)_2(SiO_4)_6$ (PDF card 83-1494). β-Ca_2SiO_4 was a predominant phase, and $Ca_{15}(PO_4)_2(SiO_4)_6$ became an accompanying phase. XRD patterns of the samples treated at 1300 and 1400 °C also show the presence of

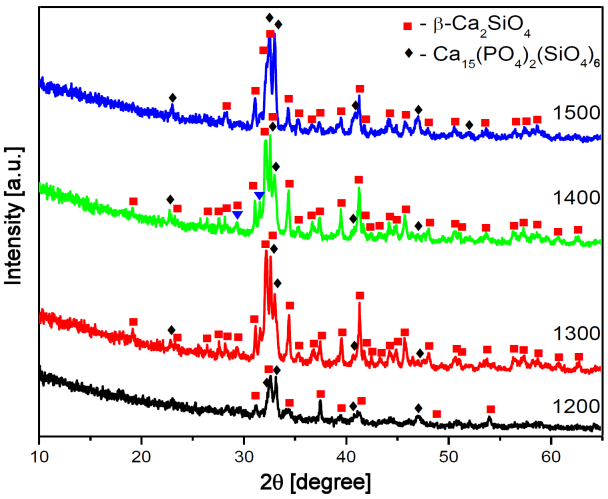

Figure 1. XRD of thermally treated CSP samples at 1200 °C, 1300 °C, 1400 °C and 1500 °C for 2 hours

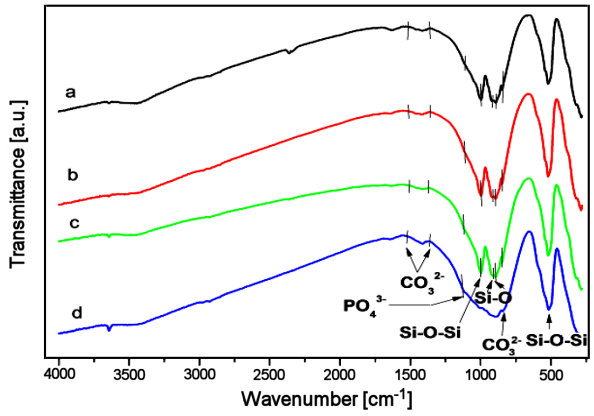

Figure 2. FTIR spectra of CSP 1200 (a), CSP 1300 (b), CSP 1400 (c) and CSP 1500 (d) samples

β-Ca_2SiO_4 and $Ca_{15}(PO_4)_2(SiO_4)_6$. In these samples β-Ca_2SiO_4 is also predominant phase. However, at 1500 °C $Ca_{15}(PO_4)_2(SiO_4)_6$ becomes predominant and β-Ca_2SiO_4 is accompanied phase.

FTIR spectra of the CSP glass-ceramics before soaking in SBF are given at Fig. 2. The presented FTIR spectra show the absorption bands corresponding to the different vibration modes of the Si–O bonds. The bands, posited at ~990 cm^{-1} can be assigned to the Si–O–Si asymmetric stretch whereas the bands at ~910–880 cm^{-1} to the Si–O symmetric strange [2,23,24]. The band at ~520 cm^{-1} could be ascribed to the Si–O–Si vibrational mode of bending. In accordance with some preliminary results, these bands could be related to the β-Ca_2SiO_4 [23,25,26]. A doublet with small intensity at ~530–610 cm^{-1} can also been observed. This doublet is characteristic of crystalline calcium phosphate (CP) and is probably due to the presence of $Ca_{15}(PO_4)_2(SiO_4)_6$ crystal phases, formed in the prepared samples [27]. The band, centred at ~1100 cm^{-1} can be assigned to the presence of $\nu_4PO_4^{3-}$ groups [9]. In accordance with our preliminary results, the bands posited at ~1530–1360 cm^{-1} and at ~840 cm^{-1} could be ascribed to the ν_3 and ν_2 CO_3^{2-} [13]. The presence of these bands is attributed to a partial carbonation process of the synthesized glass-ceramics due to the atmospheric CO_2 as a consequence of high calcium content in the prepared samples. This phenomenon was observed by Martinez *et al.* [28] for CaO-SiO_2 sol-gel glasses. In our preliminary studies we also observed the presence of CO_3^{2-} bond in the prepared ceramics in the presence of $Ca_{15}(PO_4)_2(SiO_4)_6$ as a main phase [11]. The obtained results indicated that the glass-ceramic materials consisting $Ca_{15}(PO_4)_2(SiO_4)_6$ must be kept out of atmosphere in a desiccator. Surprisingly, in the FTIR spectra of the synthesized samples treated at different temperatures the characteristic bands of $CaCO_3$ could be identified. This fact allows us to conclude that under carbonization process the role of atmospheric CO_2 could be expressed for the formation of carbonate substituted crystalline calcium phosphates.

FTIR spectra of the obtained glass-ceramics after soaking in SBF solution for 14 and 28 days are given in Figs. 3 and 4.

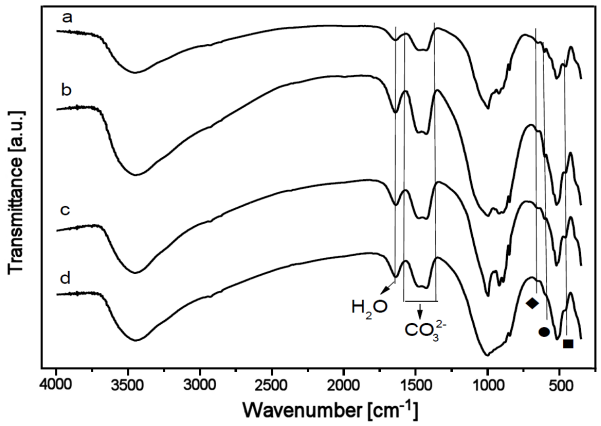

Figure 3. FTIR spectra of CSP 1200 (a), CSP 1300 (b), CSP 1400 (c) and CSP 1500 (d) samples after *in vitro* test for 14 days

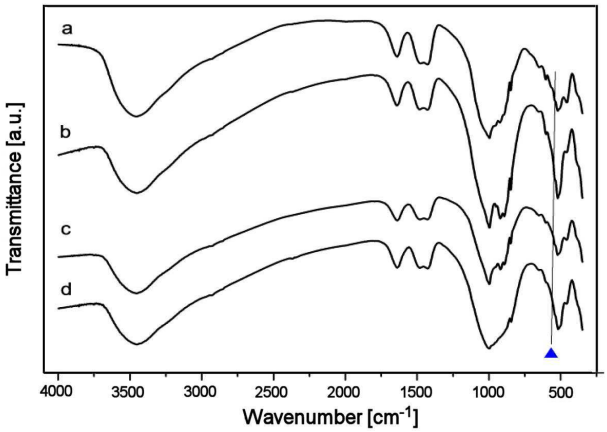

Figure 4. FTIR spectra of CSP 1200 (a), CSP 1300 (b), CSP 1400 (c) and CSP 1500 (d) samples after *in vitro* test for 28 days

For the precipitates, the observed absorption peaks showed that these were typical spectra for the carbonated hydroxyapatite, confirming that the precipitates are CO_3HA [29].

Theoretically, four vibration modes are expected for the phosphate ions in the HA spectra: ν_1 PO_4^{3-} at 961–965 cm^{-1}, ν_2 PO_4^{3-} at 460 cm^{-1}, ν_3 PO_4^{3-} at 1190–980 cm^{-1} and ν_4 PO_4^{3-} at 660–520 cm^{-1} [30,31]. In our case, three new peaks at ~651 cm^{-1} (labeled as ♦) [10,32], ~602 cm^{-1} (labeled as ●) [33–45], and 560 cm^{-1} (labeled as ▲) [3,32–45] could be ascribed to the ν_4 PO_4^{3-}. The peaks at ~453 cm^{-1} (labeled as ■) could be related to the PO_4^{3-} and Si–O–Si [46–48]. ν_3 PO_4^{3-} are visible from the absorption bands, posited at 995–997 cm^{-1} for all samples [49,50]. A phosphate vibration ν_1 PO_4^{3-} is observed in the discrete visible peak at ~940 cm^{-1}, while ν_2 PO_4^{3-} is visible at ~460 cm^{-1} for all samples [30].

It was very interesting and surprising that we did not observe the presence of intensive absorption band for CO_3^{2-} ion at ~875–878 cm^{-1} which is indicative for all CO_3HA structures [51]. From the depicted FTIR results, it is seen that in our case CO_3^{2-} could be observed at ~842 cm^{-1} as an intensive band. In accordance with Regnier *et al.* [52], the observed peak can be ascribed to the carbonate ion in the crystalline calcium phosphate lattice. Ilmen *et al.* [53] noted that the peaks in the region 842–910 cm^{-1} could be related to the ν_2 out-of-plane vibration of CO_3^{2-} in the three forms of $CaCO_3$ - calcite, aragonite and vaterite.

On the basis of the obtained FTIR results, we conclude that the crystalline calcium phosphates may be formed on the soaked surface after 14 and 28 days. Furthermore, in the presented FTIR data we could also observe the presence of intensive bands in the region ~1580–1360 cm^{-1}. These peaks could be denoted as CO_3^{2-} [3,29,33,35,36,38–41,44,46,47,54–57], thus, their presence showed that the crystalline calcium phosphates could be related to CO_3HA. The bands at ~1634 cm^{-1} are related to the H_2O in the soaked glass-ceramics [29,57].

It is well known that the apatite structure depends on its chemical compositions. There are two types of substitutions into HA lattice: CO_3^{2-} can replace PO_4^{3-} ions (B-type) and CO_3^{2-} can replace OH^- ions (A-type) [52,58–61]. For more detailed information about the type of substitution in CO_3HA formed on the surface of CSP samples after immersion in SBF solution for 14 and 28 days, the analysis by curve-fitting of the FTIR spectra in the region 1350–1600 cm^{-1} was performed, as it is visible form Fig. 5.

From the presented FTIR results four types of regions of ν_3 CO_3^{2-} were observed: 1410–1430 cm^{-1}, 1430–1460 cm^{-1}, 1460–1500 cm^{-1} and 1500–1530 cm^{-1}. The peaks position could be related with literature data as follows: for B-type CO_3HA at 1410 cm^{-1} [54,55], 1415, 1417 cm^{-1} [38,40,44,55,56], 1419, 1420–1423 cm^{-1} [3,29,33,36,39,41,46,55,57], 1437 cm^{-1} [55,57], 1449, 1455, 1458, 1459, 1460 cm^{-1} [35,39–41,55–57], 1472, 1478 cm^{-1} [3,29,47] and 1482, 1483, 1485, 1486 cm^{-1} [47], and for A-type CO_3HA at 1500, 1502, 1505–1508 cm^{-1} [46,60,62,63], 1512, 1516, 1517 cm^{-1} [19], 1525 cm^{-1} [64] and 1530, 1533 cm^{-1} [61].

On the basis of the obtained results we can conclude that B-type CO_3HA is preferentially observed on the surface of the soaked CSP samples. On the other hand, A-type CO_3HA was also detected. In addition, the band posited at 1422 and 1437 cm^{-1} could be ascribed to the A/B-type of CO_3HA [65]. Briefly, we can summarize that the synthesized and thermally treated at different temperatures CSP samples are *in vitro* bioactive in SBF solution.

Figure 6 presents SEM images for the synthesized and thermally treated CSP samples before soaking in SBF solution. As it is seen, if the dried gel is treated at 1200 °C (Fig. 6a) two type of particles can be observed: i) spherically shaped with size in the range 1–3 μm and, ii) plate-like shaped with size in the range of 5 μm. Some authors concluded that the spherical particles are characteristic for β-Ca_2SiO_4. For instance, Chrysafi *et al.* [66] postulated that these particles most probably were the reason for the stabilization of β-Ca_2SiO_4 at ambient temperature without the need of any stabilizers. The particles with plate-like morphology could be ascribed to the $Ca_{15}(PO_4)_2(SiO_4)_6$ in accordance with our preliminary results [13]. Mostafa *et al.* [6] concluded that the preparation of ceramics with this structure could be ascribed to the presence of silica in calcium phosphate structures as a function of the annealing temperature. When the temperature of thermal treatment increased, the quantity of particles with plate-like morphology also increased (Figs. 6b,d). The depicted SEM images are in a good agreement with XRD analysis of the samples. As it can be seen, the SEM image of the CSP 1400 sample is quite different. On the right corner of the SEM image we can see the presence of small globular particles with different sizes in the range 0.5–1.5 μm. These particles could be related to CO_3HA on the surface of the synthesized sample. In accordance with FTIR data presented at Fig. 2, partial carbonation process is conducted.

Figures 7 and 8 show the SEM/EDX observations of the soaked surface of the CPS samples in SBF solution for 14 and 28 days. After 14 days of soaking, the morphology of glass-ceramics surface changed distinctly with respect to that of the initial surface (Fig. 6). From the depicted SEM/EDX results (Fig. 7) it is easily seen that the mineralized surface is covered with a solid layer having small globular morphology [3,67–69]. EDX analyses indicate the presence of large amount of Ca and P with small amount of Si on the soaked surface [33]. Furthermore, Na and Mg have also been observed in traces only [3]. These ions are always present in bones, teeth and other calcified tissues. EDX revealed that for the CSP 1200 sample Ca/(P+Si) ra-

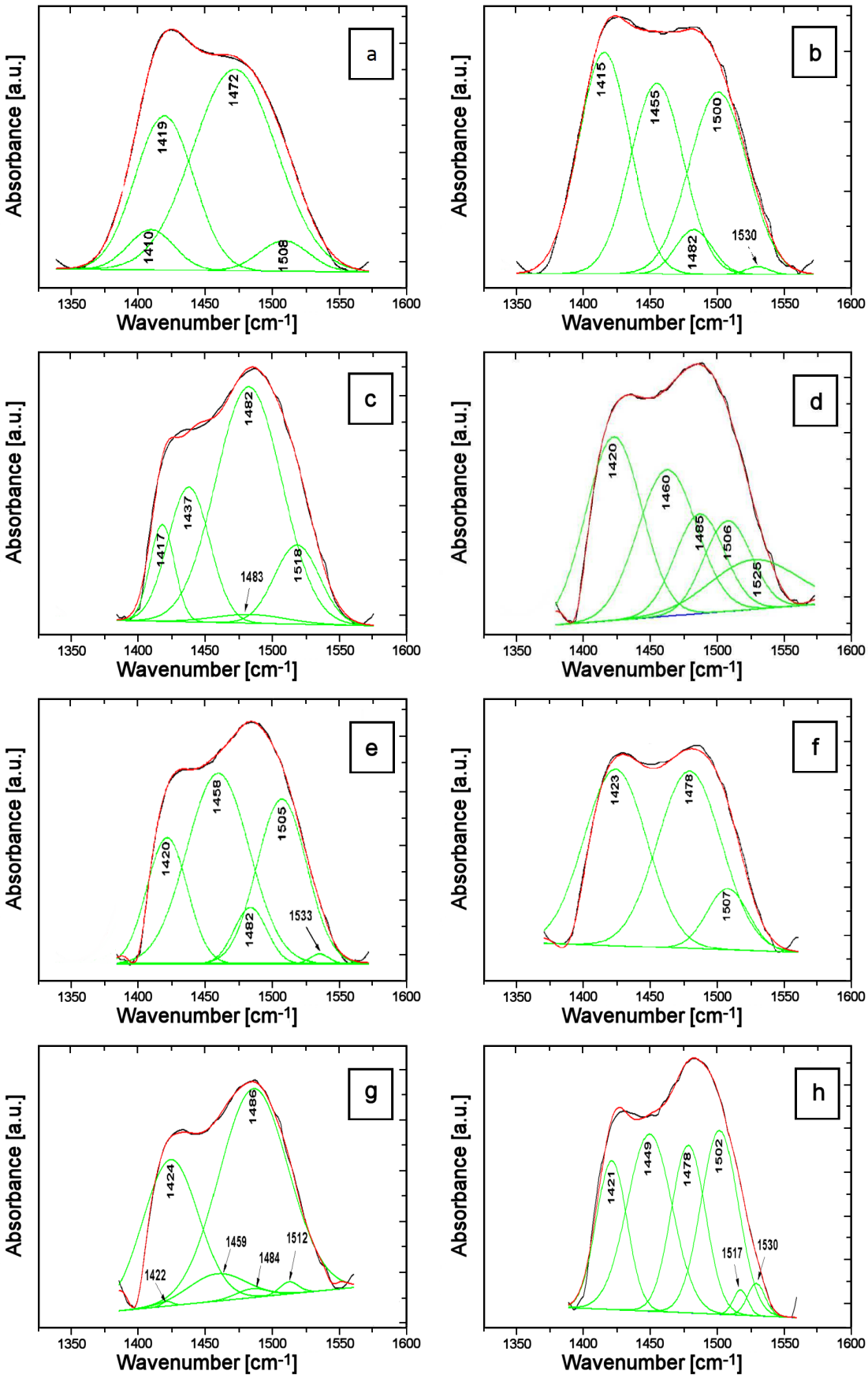

Figure 5. Curve-fitting of the FTIR spectra of samples treated at different temperatures and soaked in SBF for various times: CSP 1200 for 14 (a) and 28 (e) days, CSP 1300 for 14 (b) and 28 (f) days, CSP 1400 for 14 (c) and 28 (g) days, CSP 1500 for 14 (d) and 28 (h) days

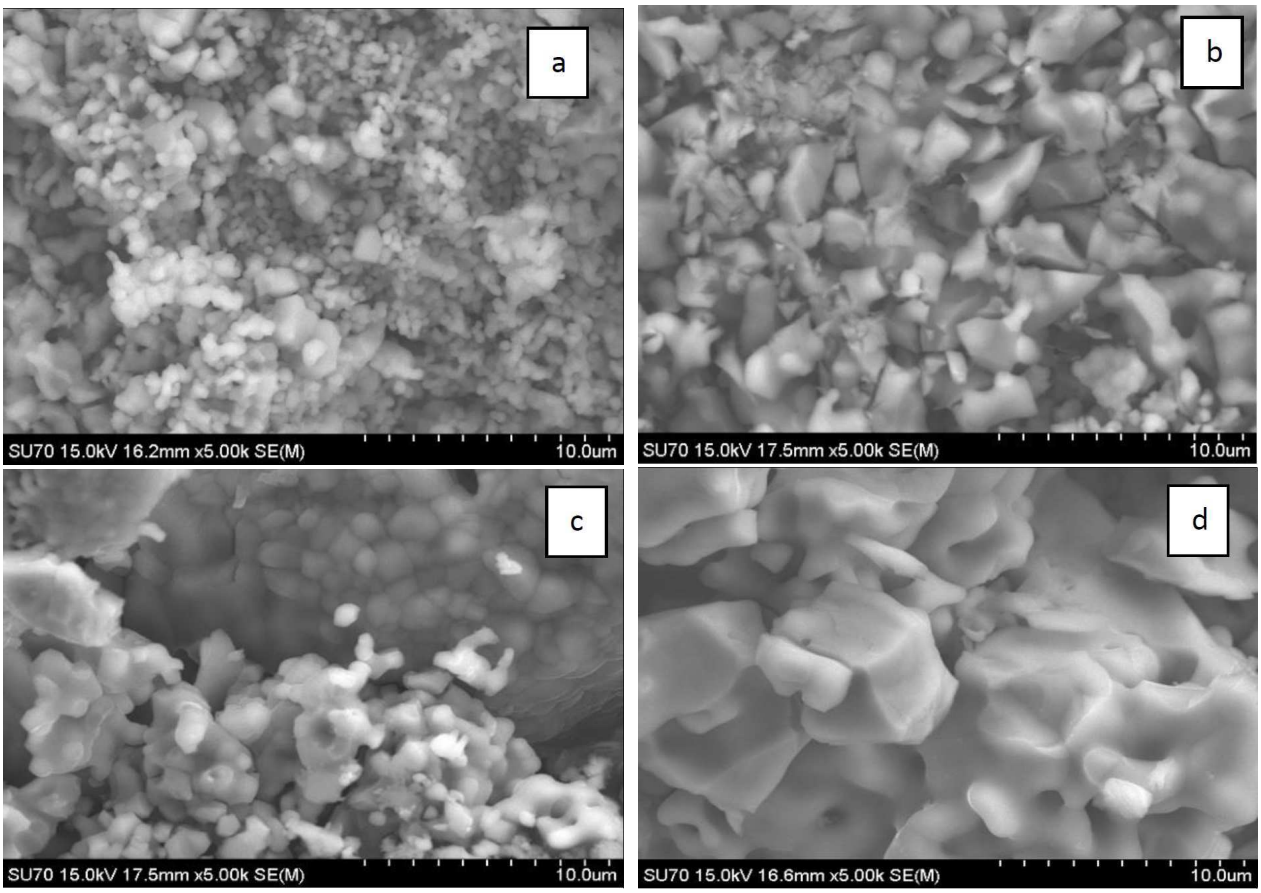

Figure 6. SEM of thermal treated CSP 1200 (a), CSP 1300 (b), CSP 1400 (c) and CSP 1500 (d) samples before *in vitro* test

tio (in wt.%) was 1.43. The observed ratio is less than the stoichiometric value of 1.67 for pure HA structures. This is because CO_3^{2-} ions are located in PO_4^{3-} sites [39]. For CSP 1300 and CSP 1500 samples Ca/(P+Si) ratio is 1.83 and 1.74, respectively. As it can be seen, the presented ratio is much higher than the stoichiometric ratio. Deviation of Ca/(P+Si) ratio could be related to the cation substitutions at the Ca^{2+} sites by Mg^{2+} or Na^+, substitution at PO_4^{3-} sites by CO_3^{2-} and/or SiO_4^{4-}, or a combination of these substitutions [70]. Finally, CPS 1500 sample proved Ca/(P+Si) ratio of 1. 61 after 14 days of soaking [71].

After 28 days of immersion SEM (Fig. 8) no significant changes in the layer morphology was detected. As it can be seen from the presented SEM images, the glass ceramic surface was covered by a layer of spherical particles less than ~10 μm in diameter. On the other hand, the covered surface is more compact and the size of the visible macropores decreases [72]. EDX results revealed that Ca/(P+Si) ratio decreased in the order CSP 1200 (1.65) > CSP 1300 (1.57) > CSP 1400 (1.40) > CSP 1500 (1.28). From EDX results we can conclude that HA, and Ca-def. HA was formed on the immersed samples.

Figures 9 and 10 show the changes in the concentrations of Ca, P and Si in SBF solutions, measured by ICP-AES, after soaking for 14 and 28 days. From the presented ICP-AES results, it is obvious that the concentration of SBF solutions changed remarkably after 14 days. Compared with the quantity of these ions in SBF solution (sample 1 in both figures), the Ca and Si concentrations increased rapidly [73]. On the contrary, the concentration of P decreased from 35 mg/l in SBF solution to <1 mg/l in both solutions. After 28 days of immersion (Fig. 10), the Ca concentrations increased, while Si concentrations decreased. The increasing of Ca ions with increasing of soaking time could be related to a faster consumption of this ion, during the crystalline carbonate apatite formation on the surface of the soaked samples [23]. On the other hand, the decreasing of P and Si concentrations during the soaking periods could be ascribed to the consumption of these ions from SBF solutions.

As it is known, the nucleation and growth of a crystalline apatite layer after soaking in SBF on CaO-SiO_2 sol-gel glass-ceramics was proposed by Ebisawa *et al.* [74]. Some authors concluded that an interexchange between Ca ions of the sample and the solution H_3O^+ takes place, giving rise to the formation of Si-OH groups on the glass-ceramic surface that induce the apatite nucleation [75]. Gandolfi *et al.* proved that reaction between Ca ions with H^+ or H_3O^+ could form the aqueous mixing solution to form a solid-liquid interface [76]. Furthermore, the reaction between Ca and OH ions gives $Ca(OH)_2$ which creates high alkaline environment [77]. On the basis of these hydration processes, cation

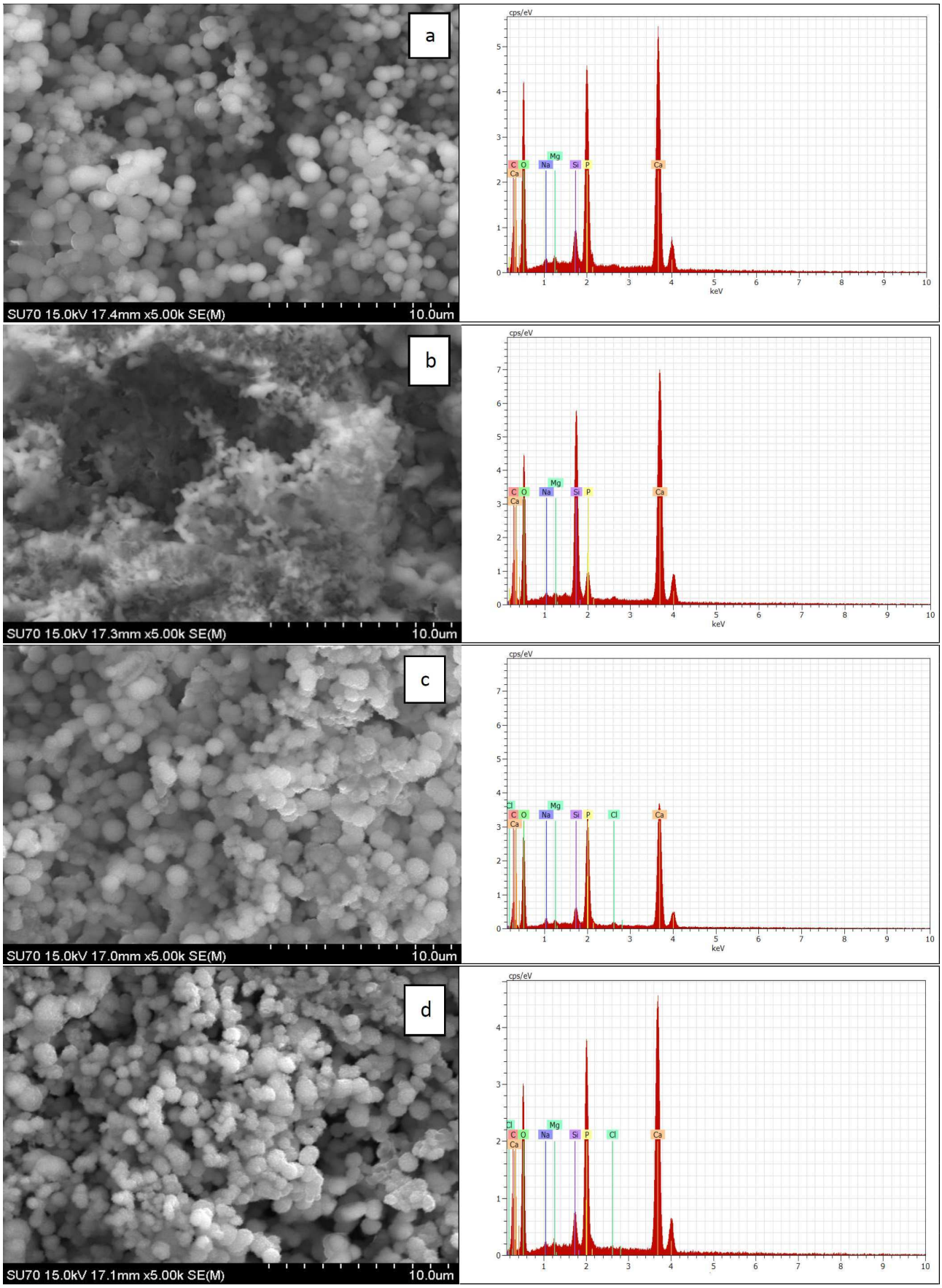

Figure 7. SEM/EDX of CSP 1200 (a), CSP 1300 (b), CSP 1400 (c), and CSP 1500 (d) samples after *in vitro* test in SBF for 14 days

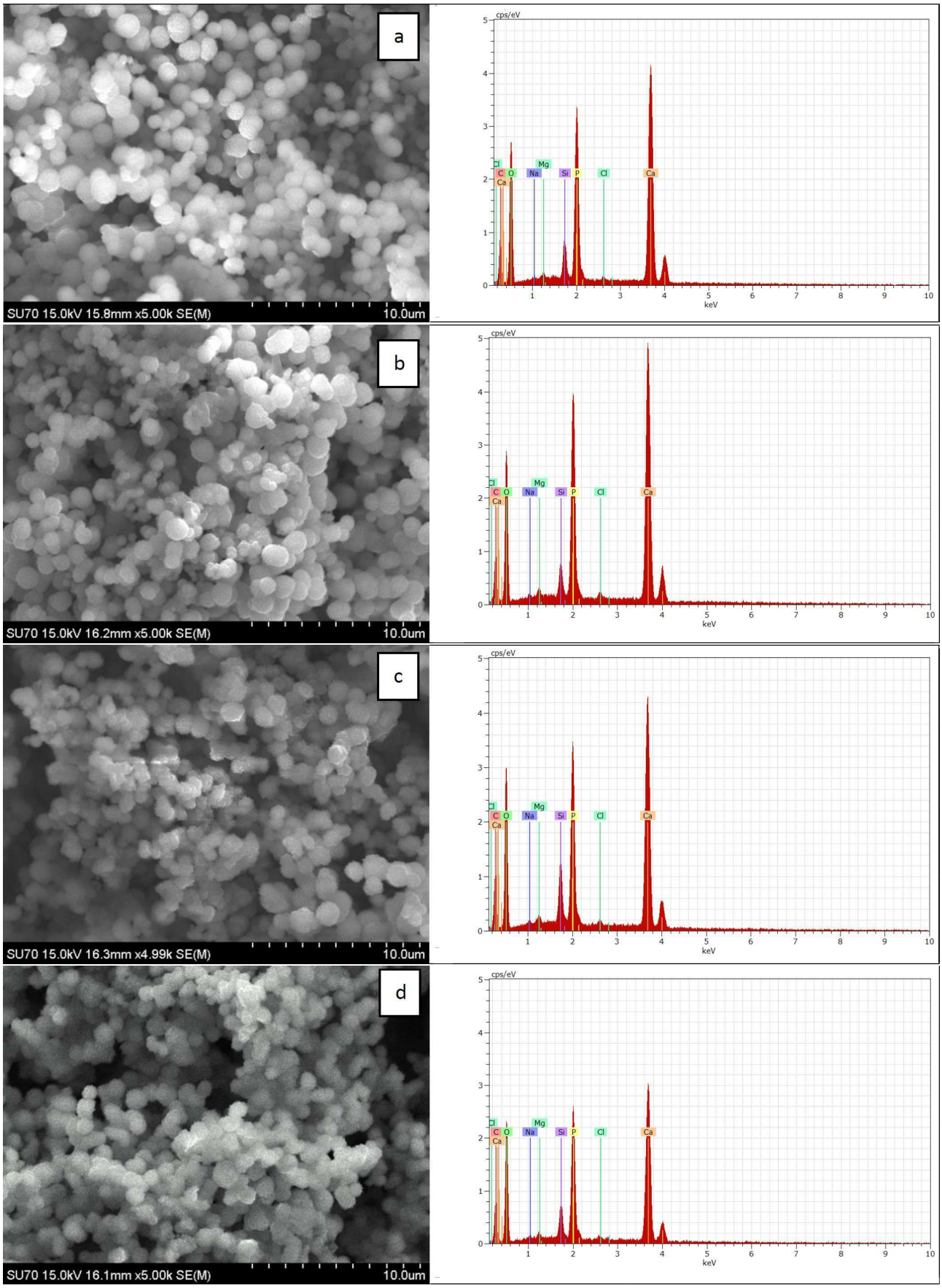

Figure 8. SEM/EDX of CSP 1200 (a), CSP 1300 (b), CSP 1400 (c), and CSP 1500 (d) samples after *in vitro* test in SBF for 28 days

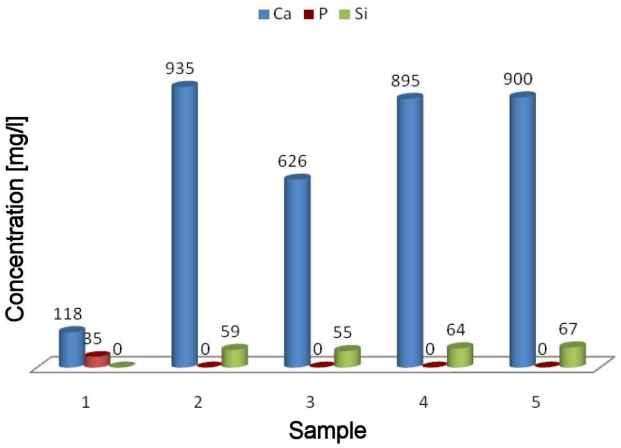

Figure 9. ICP-AES for SBF (1), CSP 1200 (2), CSP 1300 (3), CSP 1400 (4) and CSP 1500 (5) samples after soaking in SBF for 14 days

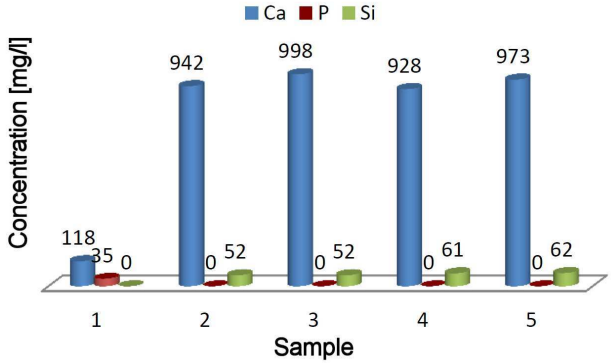

Figure 10. ICP-AES for SBF (1), CSP 1200 (2), CSP 1300 (3), CSP 1400 (4) and CSP 1500 (5) samples after soaking in SBF for 28 days

exchange increases the OH concentration of the SBF solution [77]. In accordance with Richardson [78], the surface of calcium silicate is attached by OH ions, resulting in hydration of SiO_4^{4-} groups in alkaline environment. In our case this leads to the formation of C–S–H (calcium silicate hydrate) phase on the surface of the immersed particles [14]. C–S–H is a porous highly water containing silicate gel layer which contains Si–OH groups [78]. Then it could bind with Ca ions to produce negatively charged SiO^- groups [79]. These ions could react with Ca ions to produce $SiO^- \cdots Ca^{2+}$ fragments and form ACP [80].

On the basis of the obtained results we can conclude that silicon doped carbonate containing hydroxyapatite could be formed on the synthesized samples after in vitro test in SBF solution for 14 and 28 days in static conditions.

IV. Conclusions

The novel glass-ceramics in the $CaO\text{-}SiO_2\text{-}P_2O_5$ system have been synthesized by a polystep sol-gel method. After thermal treatment at 1200 °C of the dried samples, XRD proved the presence of β-Ca_2SiO_4 and $Ca_{15}(PO_4)_2(SiO_4)_6$. After increasing the temperature of the thermal treatment to 1500 °C, $Ca_{15}(PO_4)_2(SiO_4)_6$ became a predominant phase. FTIR of the thermal treated at different temperatures glass-ceramics showed the presence of basic absorption bands corresponding to Si–O–Si and PO_4^{3-} modes. On the other hand, the presence of bands at ~1530–1360 cm^{-1} and at ~840 cm^{-1} leads us to conclude that the partial carbonation process is conducted, i.e. the synthesized glass-ceramics must be kept in a desiccator. SEM of the synthesized samples depicts the presence of particles with different morphology. The particles with plate-like shaped type could be ascribed to $Ca_{15}(PO_4)_2(SiO_4)_6$.

After *in vitro* test for bioactivity for 14 and 28 days FRIR depicted that A-, B-, and A/B-type CO_3HA can be detected. Moreover, B-type CO_3HA was preferentially precipitated on the soaked surfaces. SEM proved that the glass ceramic surfaces were covered by a layer of spherical particles. ICP-AES measurements lead us to conclude that silicon containing carbonate hydroxyapatite (Si–CO_3HA) can be formed on the soaked surface.

References

1. S.F. Hulbert, L.L. Hench, D. Forbers, L.S. Bowman, "History of bioceramics", *Ceram. Int.*, **8** [4] (1982) 131–140.
2. E.S. Thian, J. Huang, M. Vickers, S. Best, Z. Barber, W. Bonfield, "Silicon-substituted hydroxyapatite (SiHA): A novel calcium phosphate coating for biomedical applications", *J. Mater. Sci.*, **41** (2006) 709–714.
3. S.V. Dorozhkin, "In vitro mineralization of silicon containing calcium phosphate bioceramics", *J. Am. Ceram. Soc.*, **90** [1] (2007) 244–249.
4. A. Aminian, M. Solati-Hashjin, A. Samadikuchaksaraei, F. Bakhshi, F. Gorjipour, A. Farzadi, F. Moztarzadeh, M. Schmücker, "Synthesis of silicon-substituted hydroxyapatite by a hydrothermal method with two different phosphorous sources", *Ceram. Int.*, **37** [4] (2011) 1219–1229.
5. K. Nakata, T. Kubo, Ch. Numako, T. Onoki, A. Nakahira, "Synthesis and characterization of silicon-doped hydrohyapatite", *Mater. Trans.*, **50** [5] (2009) 1046–1049.
6. N.Y. Mostafa, A.A. Shaltout, L. Radev, H.M. Hassan, "In vitro surface biocompatibility of high-content silicon-substituted calcium phosphate ceramics", *Cent. Eur. J. Chem.*, **11** [2] (2013) 140–150.
7. S. Serena, M.A. Sainz, A. Caballero, "Single-phase silicocarnotite synthesis in the subsystem $Ca_3(PO_4)_2$–Ca_2SiO_4", *Ceram. Int.*, **40** [6] (2014) 8245–8252.
8. E.M. Carlisle, "Silicon: A possible factor in bone calcification", *Science*, **16** (1970) 279–280.
9. M.R.T. Filgueiras, G. La Torre, L.L. Hench, "Solution effects on the surface reactions of three bioactive glass compositions", *J. Biomed. Mater. Res.*, **27** [12] (1993) 1485–1493.

10. Ch. Ohtsuki, T. Kokubo, T. Yamamuro, "Mechanism of apatite formation on CaO-SiO_2-P_2O_5 glasses in a simulated body fluid", *J. Non-Cryst. Solids*, **143** (1992) 84–92.
11. L. Radev, V. Hristov, I. Michailova, B. Samuneva, "Sol-gel bioactive glass-ceramics Part I: Calcium phosphate silicate/wollastonite glass-ceramics", *Cent. Eur. J. Chem.*, **7** [3] (2009) 317–321.
12. L. Radev, V. Hristov, I. Michailova, B. Samuneva, "Sol-gel bioactive glass-ceramics Part II: Glass-ceramics in the CaO-SiO_2-P_2O_5-MgO system", *Cent. Eur. J. Chem.*, **7** [3] (2009) 322–327.
13. L. Radev, V Hristov, I. Michailova, M. Helena V. Fernandes, I. Miranda M. Salvado, "In vitro bioactivity of biphasic calcium phosphate silicate glass-ceramic in CaO-SiO_2-P_2O_5 system", *Process. Appl. Ceram.*, **4** [1] (2010) 15–24.
14. L. Radev, V. Hristov, I. Michailova, M. H. V. Fernandes, I.M.M. Salvado, "Collagen/silicocarnotite composites, cross-linked with chondroitin sulphate: in vitro bioactivity", *Process. Appl. Ceram.*, **5** [3] (2011) 161–170.
15. L. Radev, V. Hristov, B. Samuneva, G. Apostolov, "Organic/inorganic bioactive materials Part I: Synthesis, structure and in vitro assessment of collagen/silicocarnotite biocoatings", *Cent. Eur. J. Chem.*, **7** [4] (2009) 702-710.
16. L. Radev, N.Y. Mostafa, I. Michailova, I.M.M. Salvado, M.H. V. Fernandes, "In vitro bioactivity of collagen/calcium phosphate silicate composites, cross-linked with chondroitin sulfate", *Int. J. Mater. Chem.*, **2** [1] (2012) 1–9.
17. L. Radev, M.H.V. Fernandes, I.M.M. Salvado, "Organic/Inorganic bioactive materials Part III: in vitro bioactivity of gelatin/silicocarnotite hybrids", *Cent. Eur. J. Chem.*, **7** [4] (2009) 721–730.
18. L. Radev, V. Hristov, M.H.V. Fernandes, I.M.M. Salvado, "Organic/inorganic bioactive materials Part IV: In vitro assessment of bioactivity of gelatin-calcium phosphate silicate/wollastonite hybrids", *Cent. Eur. J. Chem.*, **8** [2] (2010) 278–284.
19. L. Radev, T. Gerganov, H. Georgiev, A. Kolev, V. Vassileva, R. Iankova, E. Cholakova, "Silk fibroin/calcium phosphate silicate composites: In vitro bioactivity", *Int. J. Mater. Chem.*, **3A** (2013) 8–15.
20. T. Kokubo, H. Kushitani, S. Sakka, T. Kitsugi, T. Yamamuro, "Solutions able to reproduce in vivo surface-structure changes in bioactive glass-ceramic A-W", *J. Biomed. Mater. Res.*, **24** [6] (1990) 721–734.
21. F. Muller, M. Bottino, L. Muller, V. Henriques, U. Lohbauer, A. Bressiani, J. Bressiani, "In vitro apatite formation on chemically treated (P/M) Ti-13Nb-13Zr", *Dental Mater.*, **24** (2008) 50–56.
22. G. Falini, S. Fermani, B. Palazzo, N. Roveri, "Helical domain collagen substrates mineralization in simulated body fluid", *J. Biomed. Mater. Res. A.*, **87** [2] (2008) 470–476.
23. Z. Gou, J. Chang, J. Gao, Z. Wang, "In vitro bioactivity and dissolution of $Ca_2(SiO_3)(OH)_2$ and beta-Ca_2SiO_4 fibers", *J. Eur. Ceram. Soc.*, **24** (2004) 3491–3497.
24. M.Y. Benarchid, A. Diouri, A. Boukhari, J. Aride, I. Elkhandiri, "Hydration of iron-phosphorus doped dicalcium silicate phase", *Mater. Chem. Phys.*, **94** (2005) 190–194.
25. Z. Gou, J. Chang, W. Zhai, "Preparation and characterization of novel bioactive dicalcium silicate ceramics", *J. Eur. Ceram. Soc.*, **25** (2005) 1507–1514.
26. F. Puertas, F. Trivino, "Examinations by Infra-red spectroscopy for the polymorphs of dicalcium silicate", *Cement Concrete Res.*, **15** (1985) 127–133.
27. D. Arcos, J. Pena, M. Vallet-Regi, "Influence of a SiO_2-CaO-P_2O_5 sol-gel glass on the biactivity and controlled release of ceramic/polymer/antibiotic mixed materals", *Chem. Mater.*, **15** (2003) 4132–4138.
28. A. Martinez, I. Izquierdo-Barba, M. Vallet-Regi, "Bioactivity of a CaO-SiO_2 binary glasses system", *Chem. Mater.*, **12** [10] (2000) 3080–3088.
29. Y. Yusufoglu, M. Akinc, "Effect of pH on the Carbonate Incorporation into the hydroxyapatite prepared by an oxidative decomposition of calcium-EDTA chelate", *J. Am. Ceram. Soc.*, **91** [1] (2008) 77–82.
30. I. Rehman, W. Bonfield, "Characterization of hydroxyapatite and carbonated apatite by photo acoustic FTIR spectroscopy", *J. Mater. Sci.: Mater. Med.*, **8** (1997) 1–4.
31. I.R. Gibson, I. Rehman, S.M. Best, W. Bonfield, "Characterization of the transformation from calcium-deficient apatite to beta-tricalcium phosphate", *J. Mater. Sci.: Mater. Med.*, **12** (2000) 799–804.
32. K. Lin, J. Chang, R. Cheng, "In vitro hydroxyapatite forming ability and dissolution of tobermorite nanofibers", *Acta Biomater.*, **3** (2007) 271–276.
33. E. Dietrich, H. Oudadesse, A. Lucas-Girot, M. Mami, "In vitro bioactivity of melt-derived glass 46S6 doped with magnesium", *J. Biomed. Mater. Res.*, **88A** (2009) 1087–1096.
34. D. Lukito, J.M. Xue, J. Wang, "In vitro bioactivity assessment of 70 (wt.) % SiO_2–30 (wt.) % CaO bioactive glasses in simulated body fluid", *Mater. Lett.*, **59** [26] (2005) 3267–3271.
35. Y. Zhang, J. Lu, "A simple method to tailor spherical nanocrystal hydroxyapatite at low temperature", *J. Nanoparticle Res.*, **9** [4] (2007), 589–594.
36. I. Hofmann, L. Müller, P. Greil, F. A. Müller, "Precipitation of carbonated calcium phosphate powders from a highly supersaturated simulated body fluid solution", *J. Am. Ceram. Soc.*, **90** [3] (2007) 821–824.
37. A. Cüneyt Taş, "Molten salt synthesis of calcium hydroxyapatite whiskers", *J. Am. Ceram. Soc.*, **84** [2] (2001) 295–300.

38. A. Ślósarczyk, Z. Paszkiewicz, A. Zima, "The effect of phosphate source on the sintering of carbonate substituted hydroxyapatite", *Ceram. Int.*, **36** [2] (2010) 577–582.
39. Ch. Li, Sh. Liu, G. Li, J. Bai, W. Wang, Q. Du, "Hydrothermal synthesis of large-sized hydroxyapatite whiskers regulated by glutamic acid in solutions with low supersaturation of precipitation", *Adv. Powder Technol.*, **22** [4] (2011) 537–543.
40. Q. He, Zh. Huang, Y. Liu, W. Chen, T. Xu, "Template-directed one-step synthesis of flowerlike porous carbonated hydroxyapatite spheres", *Mater. Lett.*, **61** [1] (2007) 141–143.
41. A.Y.P. Mateus, C.C. Barrias, C. Ribeiro, M.P. Ferraz, F.J. Monteiro, "Comparative study of nanohydroxyapatite microspheres for medical applications", *J. Biomed. Mater. Res.*, **86A** [2] (2008) 289–569.
42. K. Yamashita, T. Arashi, K. Kitagaki, Sh. Yamada, T. Umegaki, K. Ogawa, "Preparation of apatite thin films through rf-sputtering from calcium phosphate glasses", *J. Am. Ceram. Soc.*, **77** [9] (1994) 2243–2495.
43. X. Chen, B. Lei, Y. Wang, N. Zhao, "Morphological control and in vitro bioactivity of nanoscale bioactive glasses", *J. Non-Cryst. Solids*, **355** [13] (2009) 791–796.
44. D.P. Minh, N.D. Tran, A. Nzihou, P. Sharrock, "Carbonate-containing apatite (CAP) synthesis under moderate conditions starting from calcium carbonate and orthophosphoric acid", *Mater. Sci. Eng. C*, **33** (2013) 2971–2980.
45. Ch. Gu, D.R. Katti, K.S. Katti, "Photoacustic FTIR spectroscopy study of undisturbed human cortical bone", *Spectrochim. Acta Part A: Mol. Biomol. Spectrosc.*, **103** (2013) 25–37.
46. S. Agathopoulos, D.U. Tulyaganov, J.M.G. Ventura, S. Kannan, M.A. Karakassides, J.M.F. Ferreira, "Formation of hydroxyapatite onto glasses of the CaO-MgO-SiO_2 system with B_2O_3, Na_2O, CaF_2 and P_2O_5 additives", *Biomater.*, **27** [9] (2006) 1832–1840.
47. G.S. Pappas, P. Liatsi, I.A. Kartsonakis, I. Danilidis, G. Kordas, "Synthesis and characterization of new SiO_2-CaO hollow nanospheres by sol-gel method: Bioactivity of the new system", *J. Non-Cryst. Solids*, **354** [2-9] (2008) 755–760.
48. Â.L. Andrade, P. Valério, A.M. Goes, M. de Fátima Leite, R.Z. Domingues, "Influence of morphology on in vitro compatibility of bioactive glasses", *J. Non-Cryst. Solids*, **352** [32-35] (2006) 3508–3511.
49. E.P. Pashalis, E. DiCarlo, F. Betts, P. Sherman, R. Mendelson, A.L. Boskey, "FTIR microspectroscopic analysis of human osteonal bone", *Calcif. Tissue Int.*, **59** (1996) 480–487.
50. E. Pashalis, R. Mendelson, A.L. Boskey, "Infrared assessment of bone quality", *Clin. Orthop. Relat. Res.*, **469** (2011) 2170–2178.
51. R. LeGeros, O.R. Trautz, E. Klein, J.P. LeGeros, "Two typs of carbonate substitution in the apatite structure", *Experimentia*, **25** [1] (1968) 5–7.
52. P. Regnier, A.C. Lasaga, R.A. Berner, O.H. Han, K.W. Zum, "Mecanism of CO_3^{2-} substitution in carbonate-fluorapatite: Evidence from FTIR spectroscopy, ^{13}C NMR and quantum mechanical calculations", *Am. Mineral.*, **79** (1994) 809–818.
53. R Ilmen, U. Jaglid, "Carbon portland cement studied by diffuse reflection Fourier transform infrared spectroscopy", *Int. J. Concr. Srt. Mater.*, **7** [2] (2013) 119–125.
54. Ch. T. Zaman, A. Takeuchi, Sh. Matsuya, Q.H.M. Zaman, K. Ishikawa, "Fabrication of B-type carbonate apatite blocks by the phosphorization of free-molding gypsym-calcite composite", *Dental Mater. J.*, **27** [5] (2008) 710–715.
55. Zh. Hong, A. Liu, L. Chen, X. Chen, X. Jing, "Preparation of bioactive glass ceramic nanoparticles by combination of sol-gel and coprecipitation method", *J. Non-Cryst. Solids*, **355** [6] (2009) 368–372.
56. F. Apfelbaum, H. Diab, I. Mayer, J.D.B. Featherstone, "An FTIR study of carbonate in synthetic apatites", *J. Inorg. Biochem.*, **45** (1992) 277–282.
57. M. Cerruti, C. Morterra, "Carbonate formation on bioactive glasses", *Langmuir*, **20** [15] (2004) 6382–6388.
58. R. Santos, R. Clayton, "The carbonate content in high-temperature apatite: An analytical method applied to Apatite from the Jacupuranga alkaline complex", *Am. Mineral.*, **80** (1995) 336–344.
59. M. Fleet, X. Liu, P. King, "Accomodation of the carbonate ion in apatite: An FTIR and X-ray structure study of crystals synthered at 2-4 GPa", *Am. Mineral.*, **89** (2004) 1422–1432.
60. M. Fleet, X. Liu, "Location of type B carbomate ion in type A-B carbonate apatite synthesized at high presure", *J. Solid State Chem.*, **177** (2004) 3174–3182.
61. M. Fleet, X. Liu, "Coupled substitution of A and B carbonate in sodium-bearing apatite", *Biomater.*, **28** (2007) 916–926.
62. C. Rey, B. Collins, T. Goehi, I.R. Dickenson, M.J. Glimsher, "The carbonate environment in bone mineral: A resolution enhanced Fourier transform infrared spectroscopy study", *Calcif. Tissue Int.*, **45** (1989) 157–164.
63. H. El Feki, Ch. Rey, M. Vignoles, "Carbonate ions in apatites: Infrared investigations in the CO_3 domain", *Calcif. Tissue Int.*, **49** (1991) 269–274.
64. P. Comodi, Y. Liu, "CO_3^{2-} substitution in apatite: Further insight from new crystal-chemical data of Kasekere (Uganda) apatite", *Eur. J. Mineral.*, **12** (2000) 965–974.
65. J.P. Lafon, E. Champion, D. Barnache-Assolant, "Processing of AB-type carbonated hydroxyapatite $Ca_{10-x}(PO_4)_{6-x}(CO_3)_x(OH)_{2-x-2y}(CO_3)_y$ ceramics with controlled composition", *J. Eur. Ceram. Soc.*, **28** [1] (2008) 139–147.

66. R. Chrysafi, Th. Perraki, G. Kakali, "Sol-gel preparation of 2 $CaO \cdot SiO_2$", *J. Eur. Ceram. Soc.*, **27** (2007) 1707–1710.
67. C.-C. Chen, C.-W. Wang, N.-S. Hsueh, S.-J. Ding, "Improvent of in vitro physicochemical properties and osteogenic activity of calcium phosphate sulfate cement for bone repair by dicalcium silicate", *J. Alloys Compd.*, **585** (2014) 25–31.
68. J. Ma, C. Chen, D. G. Wang, X. G. Meng, J. Z. Shi, "In vitro degradability and bioactivity of mesoporous CaO-MgO-P_2O_5-SiO_2 glasses synthesized by sol-gel method", *J. Sol-Gel Sci. Technol.*, **54** (2010) 69–76.
69. Ch. Vaid, S. Murugavel, Ch. Das, S. Asokan, "Mesoporous bioactive glass and glass-ceramics: Influence of the local structure on in vitro bioactivity", *Micropor. Mesopor. Mater.*, **18** (2014) 46–56.
70. D.O. Costa, B.A. Allo, R. Classen, J.L. Hutter, S.J. Dixon, A.S. Rizkalla, "Control of surface topography in biomimetic calcium phosphate coatings", *Langmuir*, **28** (2012) 3871–3880.
71. M. Magallanes-Perdomo, Z.B. Luklinska, A.H. De Aza, R.G. Carrodeguas, S. de Aza, P. Pena, "Bone-like forming ability of apatite-wollastonite glass ceramics", *J. Eur. Ceram. Soc.*, **31** (2011) 1549–1561.
72. M. Vallet-Regi, A. Ramila, "New bioactive galss and changes in porosity during the growth of a carbonate hydroxyapatite layer on glass surfaces", *Chem. Mater.*, **12** (2000) 961–965.
73. D.M. Ibrahim, A.A. Mostafa, S.I. Korowash, "Chemical characterization of some substituted hydrohyapatites", *Chem. Cent. J.*, **5** [1] (2011) 74
74. Y. Ebisawa, T. Kokubo, K. Ohura, T. Yamamuro, "Bioactivity of $CaO \cdot SiO_2$-based glasses: in vitro evaluation", *J. Mater. Sci.: Mater. Med.*, **1** [4] (1990) 239–244.
75. J. Roman, S. Padilla, M. Vallet-Regi, "Sol-gel glasses as precursors of bioactive glass-ceramics", *Chem. Mater.*, **15** (2003) 798–806.
76. M.G. Gandolfi, P. Taddei, A. Tinti, C. Prati, "Apatite-forming ability (bioactivity) of ProRoot MTA", *Int. Endodon. J.*, **43** [10] (2010) 917–992.
77. J. Camilleri, "Hydration mechanisms of mineral trioxide aggregate", *Int. Endodon. J.*, **40** [6] (2007) 462–470.
78. I.G. Richardson, "The calcium silicate hydrates", *Cem. Concr. Res.*, **38** [2] (2008) 137–158.
79. X. Liu, Ch. Ding, P.K. Chu, "Mechanism of apatite formation on wollastonite coatings in simulated body fluids", *Biomater.*, **25** [10] (2004) 1755–1761.
80. L. Niu, K. Jiao, T. Wang, W. Zhang, J. Camilleri, B.E. Bergeron, H. Feng, J. Mao, J. Chen, D.H. Pashley, F.R. Tay, "A review of the bioactivity of hydraulic calcium silicate cements", *J. Dent.*, (2014) http://dx.doi.org/10.1016/j.jdent.2013.1012.1015.